Probing the Structure of $NaYF_4$ Nanocrystals using Synchrotron-Based Energy-Dependent X-ray Photoelectron Spectroscopy

Jothirmayanantham Pichaandi, Gautom Kumar Das, Noah J. J. Johnson, Tom Regier and Frank C.J.M. van Veggel

September 2014

http://dx.doi.org/10.1021/jp505646j

Probing the Structure of $NaYF_4$ Nanocrystals using Synchrotron-Based Energy- Dependent X-Ray Photoelectron Spectroscopy

Jothirmayanantham Pichaandi[1], Gautom Kumar Das[1], Noah J. J. Johnson[1], Tom Regier[2], Frank C. J. M. van Veggel[1*]

[1] Department of Chemistry, University of Victoria, P.O. Box 3065, Victoria, British Columbia, Canada, V8W 3V6

[2] Canadian Light Source Inc., University of Saskatchewan, 101 Perimeter Road, Saskatoon, SK, Canada, S7N 0X4.

* corresponding author email: fvv@uvic.ca

Abstract

Understanding the structure and chemical speciation of the synthesized lanthanide doped $NaYF_4$ nanocrystals is of paramount importance to improve and optimize their physical and chemical properties. Hence in this work we employ synchrotron-based high resolution X-ray photoelectron spectroscopy (XPS) measurements to analyze lanthanide-doped and undoped $NaYF_4$ nanocrystals. These measurements revealed that there are two doublets for the yttrium ions in the nanocrystal instead of the single doublet in case all Y^{3+} ions have the same chemical environment, generally observed around a binding energy of 160 eV (3d photoelectrons of Y^{3+}). This second doublet (binding energy ~ 157.5 eV) was convoluted with the first doublet (binding energy ~ 160 eV) and the intensity of this doublet increased with decrease in excitation x-ray energy. The second doublet was confirmed to belong to the yttrium ions as doped and undoped $NaYF_4$ nanocrystals exhibit this second peak. The peaks were deconvoluted showing that the second peak is also a doublet with the ratio of the peaks being 2:3. This is exactly the same as what we have observed for the first doublet of the 3d photoelectrons of yttrium ions. In addition, we observe an increase in intensity of the second doublet in comparison to the original 3d doublet of the yttrium ions as the excitation energy is decreased. This suggests that the second doublet is from surface yttrium ions in the $NaYF_4$ nanocrystal. To confirm our hypothesis, a shell of $NaYbF_4$ or $NaTmF_4$ was grown over the $NaYF_4$ nanocrystal and the second doublet for the yttrium ions was not observed. This is an additional confirmation that the second doublet is indeed from the surface yttrium ions. This implies that the yttriums on the surface of the nanocrystals have a (slightly) different chemical speciation than their counterparts inside the nanocrystals. We attribute the new chemical speciation of surface yttrium ions to the different chemical environment they encounter than their counterparts inside the nanocrystal.

Keywords: Nanocrystals, Lanthanides, Chemical speciation, Upconversion, Surface ions, X-ray Photo-electron Spectroscopy (XPS)

Introduction

Nanocrystals in general have attracted wide spread attention in a large number of applications ranging from electronics to contrast agents in medicine due to their unique properties at the nanometer level.[1-2] A fundamental understanding of their structure and chemical speciation will enable researchers to tune the synthesis of nanocrystals and their surface with respect to their physical properties depending on the required application.[3] This will further the understanding of the materials at the nanoscopic level. Lanthanide nanocrystals have garnered a lot of attention in the past decade due to their intrinsic optical properties (optical amplifiers, solar cells, optical imaging) stemming from the intra-4f transitions and their paramagnetic properties (MRI, permanent magnets) because of their unpaired 4f electrons.[4-5] The important aspect of lanthanide optical properties is the fact that the filled 5s and 5p orbitals shield the partially filled 4f orbitals, the emission wavelength is impervious to any major shift from the solvents, ligands, or the surrounding environment.[6] The speciality of lanthanides is the fact that they can convert two or more lower energy photons to one higher energy photon through a step-wise process at very low power densities (several to 100 mW/cm^2), which is called upconversion.[7] Upconversion is generally achieved by co-doping ytterbium with another lanthanide ion (Er^{3+}, or Ho^{3+} or Tm^{3+} ions) in a matrix. Ytterbium has only one excitation level around 980 nm and has the highest absorption cross section area (~ 10^{-20} cm^2) among all lanthanides.[6] The best possible upconversion efficiency is obtained by using $NaYF_4$ as the matrix for doping the lanthanides.[8] One of the potential applications for upconversion is the use of lanthanides in bioimaging. The primary motive for employing lanthanides for this application is that the excitation (980 nm from

Yb^{3+} ions) and emission (800 nm from Tm^{3+} ions) wavelengths lie in the region where tissue scatters light the least and the tissues have minimal autofluorescence in this region.[9-11]

A lot of development in synthesis and surface modification of lanthanide doped nanocrystals has been carried out to make them compatible for bioimaging.[12-13] In most of the reports surface quenching has been used as an argument to explain the decrease in optical efficiency of the lanthanide doped nanocrystals after surface modification.[14-16] However, there has been no concrete evidence to back up this argument other than the indirect evidence obtained by comparing core and core-shell nanocrystals. Furthermore, when ligand exchange is performed the surface may undergo etching which can sometimes be seen in TEMs of ligand-exchanged particles. This obviously changes the stoichiometry of the nanocrystal surface and thus may lead to (subtle) crystal field effects on the Ln^{3+} ions. This could also introduce more and new surface quenching sites. All the above points necessitate the fact that the surface of the nanocrystals needs to be well understood in order to modify them for further applications like biolabeling, magnetic resonance imaging (MRI), and mass cytometry. In addition the doping of lanthanides in a matrix could also potentially influence the surface, i.e. crystal field effects, etc., of the synthesized nanocrystals when compared to the undoped matrix.

On the above mentioned aspects, very few attempts have been made to understand the structure and the surface of these nanocrystals through fundamental characterization techniques like X-ray Photo-electron Spectroscopy (XPS), and X-ray absorption spectroscopy (XAS).[17-20] Our previous studies have employed energy-dependent XPS measurements to study the doping distribution and the core/shell structure of the lanthanide doped nanocrystals. Our group has provided evidence for the core/shell structure of the $NaYF_4/NaGdF_4$ by using synchrotron-based energy-dependent X-ray photoelectron spectroscopy (XPS).[21-22] The structures of lanthanide trifluorides

like LaF_3/NdF_3, LaF_3/GdF_3, and NdF_3/LaF_3 were also studied with synchrotron-based energy-dependent XPS.[23] When we studied the doping distribution of Nd^{3+}, Tb^{3+}, and Y^{3+} ions in $NaGdF_4$ matrix we found that that the distribution was not isotropic, as could have been expected based on the fact that the Ln^{3+} ions are chemically very similar.[24] All of our previous reports strongly imply that high resolution XPS measurements at different excitation energies can potentially reveal detailed information about the structure and the surface of the nanocrystals. Our prior results from LaF_3 nanocrystals doped with Eu^{3+} ions showed that the surface Eu^{3+} ions are different from the bulk which was deduced by the lifetime and luminescence of Eu^{3+} ions. This is again an indirect evidence for the fact that surface ions could be different from their counterparts.[14] This motivated us to investigate the lanthanide doped $NaYF_4$ nanocrystals with high resolution XPS measurements to obtain valuable information on the surface structure of the nanocrystals. Furthermore, the technique employed to investigate the surface structure of the nanocrystals is also very generic. Our current report examines in particular the surface of the lanthanide doped and undoped $NaYF_4$ nanocrystals which revealed that the surface yttrium ions are different from the yttrium ions inside the nanocrystals. This is ascertained by the fact that we observe two doublets for the 3d photoelectrons of yttrium ions instead of one. The second doublet was not observed when a shell was grown over the $NaYF_4$ which provided additional evidence for the fact that the second doublet is from surface yttrium ions and not due to a core/shell structure. We thus provide concrete evidence for the fact that the surface yttrium ions have a different chemical speciation when compared to the yttrium ions inside the nanocrystal.

Results and Discussion

Synthesis and Characterization

The synthesis of nanocrystals was done according to procedure developed by our group.[11] The high reaction temperature yields monodisperse, and highly crystalline nanocrystals. The TEMs in Figure 1A &B shows a size and size distribution of nanocrystals of 18 ± 2 nm. Using the XRD peaks (at 44 and 46 degrees, Figure 1D) and Scherrer's equation, the calculated crystallite size (~ 20 and ~21 nm) corroborates with the size obtained from TEM. The XRD measurements show that these nanocrystals are of hexagonal phase of $NaYF_4$ which has been known to be the most efficient upconverting matrix. The optical measurements in Figure 1C show that 800 nm is the most dominant emission wavelength which is the desired wavelength for bioimaging application. The monodispersity of the nanocrystals is very essential for our synchrotron-based energy-dependent XPS measurements because these are ensemble measurements which will reflect the entire sample rather than just one nanocrystal. Our prior experience has shown that the amount of dopants in the nanocrystal is, as a rule of thumb, very similar to the reaction mixture.[25] The dopants employed here are thulium and ytterbium. The (nominal) doping percentages were of the order of 20 atom percent. This doping level was chosen to facilitate a good signal to noise ratio in the XPS measurements. The doping level of ytterbium reflects the amount generally employed for the upconversion process. On the other hand, the thulium doping level is quite high when compared to the levels (0.3 to 2 atom percent) used for upconversion, but this was necessary because earlier measurements with such low Tm^{3+} concentrations gave no reliable signal.

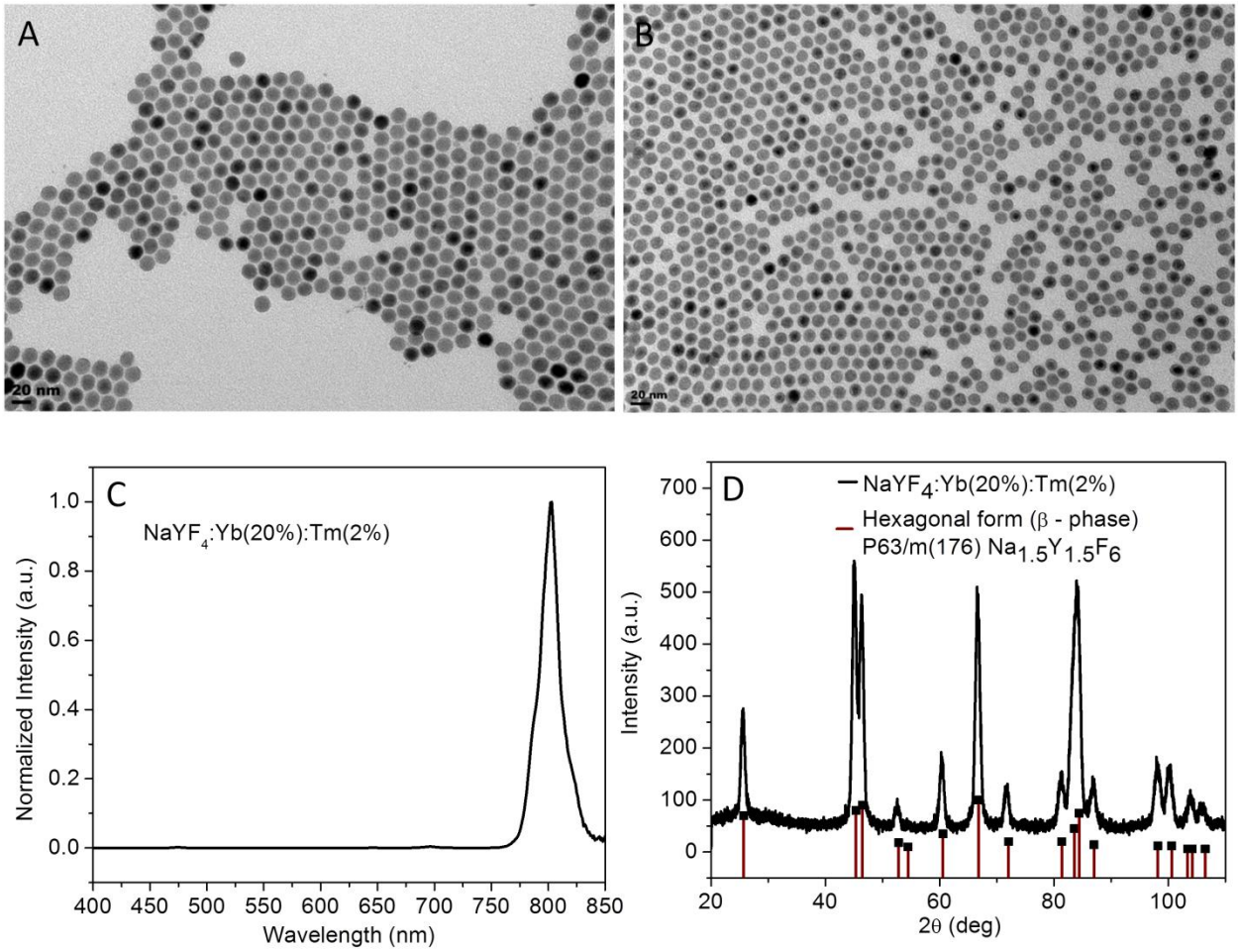

Figure 1. TEM of (A) $NaYF_4$:Yb(20%):Tm(2%); (B) TEM of $NaYF_4$:Yb(20%); (C) Luminescence Spectrum of $NaYF_4$:Yb(20%):Tm (2%) at 150 W/cm^2 (D) XRD of $NaYF_4$:Yb(20%):Tm(2%)

Energy-dependent X-ray photoelectron spectroscopy on doped and undoped $NaYF_4$ nanocrystals

The XPS spectrum of $NaYF_4$ doped with Yb^{3+} and Tm^{3+} was measured at excitation energy of 1000 eV where we can observe peaks for sodium, gold (of the foil and used as calibration), yttrium, carbon, oxygen, and fluorine. The sample was drop casted on to the gold foil whose photoelectron peaks from the 4f electrons of gold ($4f_{7/2}$ – 84 eV, $4f_{5/2}$ – 88 eV) were used as the reference peaks (Figure S1). With respect to the gold peaks as calibration, the binding energy peaks at ~ 74 eV, ~ 95 and 98 eV, ~ 172 eV (doublet), ~ 296 eV, ~ 540 eV (doublet), and 700 eV belong to sodium (2p), gold (4f), yttrium (3d), carbon (1s), oxygen (1s) and fluorine (1s), respectively.[17] The 3d peaks around 172 eV observed for yttrium from the $NaYF_4$ nanocrystals is one we are interested in studying as they exhibit a strong signal to noise ratio. The binding energies mentioned above for various elements are from the raw spectrum before any correction made with the calibration from the gold peaks. The yttrium ion exhibits its typical doublet for the 3d electrons which can clearly be observed in Figure 2. The peaks around 172 to 175 eV are also from yttrium, because these materials do not have any Ln^{3+} dopant ions. These two peaks must belong to yttrium as it is observed with doped and undoped yttrium samples and the rest of the elements oxygen, fluorine, sodium, carbon do not have any peaks around these binding energies. Moreover, the binding energy of Yb^{3+} and Tm^{3+} ions did not match with that of the reported values at ~ 180 and ~ 190 eV.[26] This validates that the peaks are definitely from Y^{3+} ions and not from the 4d photoelectrons of Yb^{3+} or Tm^{3+} ions. These peaks could be shake-up peaks of the 3d yttrium doublets observed around 160 eV. The 3d electrons of the yttrium ions exhibit a doublet which belongs to $3d_{5/2}$ and $3d_{3/2}$. The higher binding energy and higher intensity peak in the doublet is the $3d_{5/2}$ (159.5 eV) and the other one belongs to the $3d_{3/2}$ peak (161.6 eV).

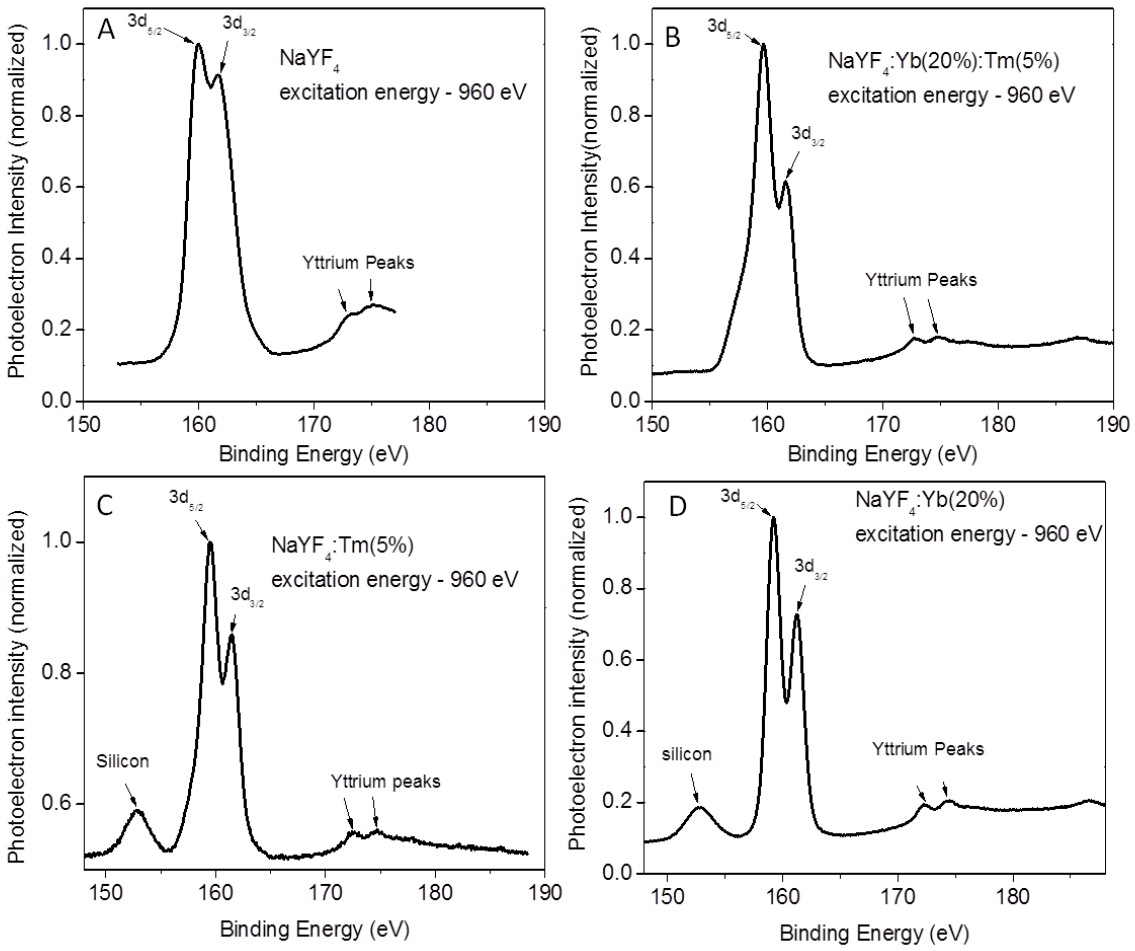

Figure 2. XPS spectra of doped and undoped $NaYF_4$ at excitation energy of 960 eV. The peak around 161 and 163 eV belong to $3d_{5/2}$ and $3d_{3/2}$ of Y^{3+}. The peak around 155 eV in the C&D spectra belong to 2s orbital of silicon.

There is another peak around 153 eV (Figure 2C & D) which belongs to silicon which comes from the fact it comes from the glassware we use for synthesizing the nanocrystals.[17] If we use brand new glassware for each synthesis the silicon peak can be avoided. This observation suggests that the synthesis leads to etching of the glassware, which might be a result of the high

temperature and the fact that fluoride is present in the reaction mixture. In Figure S1 and Figure 2 an additional peak at a slightly lower binding energy when compared to the yttrium 3d doublet (~160 eV, mentioned as first doublet from now on) is also observed. This second photoelectron peak is convoluted with the 3d doublet of the yttrium ions. The primary factor to note here is that the intensity of this doublet changes with the excitation energy. As the excitation energy is decreased from 960 to 480 eV the intensity of the second peak for yttrium increases in a relative sense. At higher excitation energies like 960 eV the second peak is seen as a shoulder to the first doublet. However, as the excitation energy is decreased the second peak is observed clearly instead of being a shoulder to the first doublet (Figure 3A and S3). If we carefully look at Figure S4 the width of the first doublet is around 4 to 5 eV, however in Figure S5 with the second peak the width has increased to about ~ 9 eV. The width did not exactly double as it should, due to the fact that the peaks are convoluted making them hard to unravel.

Furthermore, the second peak has one peak around 157.5 eV and another peak around 159.5 eV. The second peak around 159.5 eV seems to be convoluted with the $3d_{5/2}$ peak of first doublet (Figure S5) from yttrium. When the spectra at 920 and 840 eV are compared the second peak observed as a shoulder at 920 eV excitation energy is a doublet which can be clearly seen in the 840 eV. Other than yttrium none of the elements in the nanocrystal have binding energies in this region to generate a photoelectron peak. Hence, we attribute this second peak also to 3d photoelectrons of yttrium ions as they are so close to the first doublet of the 3d photoelectrons of yttrium ions. This suggests that there are two types of yttrium ions in the nanocrystals which have different chemical speciation. If the second peak is from 3d photoelectrons of yttrium then it should be a doublet as well. The combined peak width of the original and second photoelectron peak is twice that of the first doublet which strongly implies that the second peak could also be a

doublet. In order to see the second doublet they had to be deconvoluted to be observed separately. The fitting was done with the basic premise that there are two doublets in those peaks observed. From Figure 4A&B we can clearly observe that two doublets fit the raw peaks very well. We also find that when the peaks are fitted, the ratio of each doublet is around 2 to 3. The fitted parameters are shown in the supporting information in table 1, 2 and 3. Our inference from the results is that the second peak is also a doublet is further confirmed when two doublets fitted the raw peaks very well (Figure 4A &B). As this second peak is observed for both doped and undoped $NaYF_4$ nanocrystals it lends additional support to our argument that it is from yttrium ions. Only core/shell nanocrystals exhibit results where the shell material's photoelectron intensity is higher than the core at low excitation energies and vice versa at high excitation energies. A similar result observed for the $NaYF_4$ nanocrystals strongly implies that it is either due to the surface ions or a core/shell structure. We hypothesise that the second peak is from surface yttrium ions due to the fact that the second peak is just a small shoulder at high excitation energies. Another argument in favour of our hypothesis, which can be made is that formation of a core/shell structure is highly unlikely in-case of undoped $NaYF_4$ nanocrystals as its a pure matrix with no dopants.

Moreover, if the second peak is indeed from surface yttrium ions then the peak should disappear if a shell is grown over the core $NaYF_4$ nanocrystal. On the other hand, if the nanocrystal has a core/shell structure, the second peak will be observed even after a second shell is grown. To test our hypothesis a shell was grown over the $NaYF_4$ nanocrystal. The essential factor to consider while deciding the material for shell is that, the shell grows epitaxially and conformally over the core nanocrystals. This is an important criterion as we want to make sure that the shell coats the core nanocrystals uniformly and completely. Moreover the shell material has to be different from

that of yttrium so that we can distinguish it clearly. We chose ytterbium and thulium as shell materials as we had already utilized $NaYF_4$ nanocrystals doped with these two elements. This might also shed light on where the 4d binding energy peaks of ytterbium and thulium actually are, as we did not observe any signal for them when they are doped in the nanocrystal. The core/shell nanocrystals were grown using the procedure developed by our group. The TEM images in Figures S6 and S7 shows that the shell is centrosymmetric and has been uniformly coated over the nanocrystals. In order to confirm that the second doublet is from the surface ions the XPS spectrum for $NaYF_4/NaYbF_4$ and $NaYF_4/NaTmF_4$ core/shell nanocrystals were measured. The XPS spectra for the core/shell $NaYF_4/NaYbF_4$ or $NaYF_4/NaTmF_4$ nanocrystals did not show a second doublet for the yttrium ions in addition to the first doublet observed for the 3d electrons. A single doublet for Y^{3+} ions was observed in both cases which can be observed in Figure 4C. We expected the 3d doublets from the yttrium ions to exhibit a 2 to 3 ratio, which is what we observed when the peaks were fitted. The presence of a single doublet from the core/shell nanocrystals confirmed our hypothesis that the second doublet observed for doped and undoped $NaYF_4$ nanocrystals is indeed from 3d photoelectrons of surface yttrium ions and not due to a core/shell structure. The different chemical speciation observed for yttrium ions could also be due to following possibilities: 1) yttrium ions could be surrounded by oleates; 2) presence of surface defects. Additionally, the second doublet observed is definitely not due to the influence of dopants which is confirmed from the fact that it is observed with undoped $NaYF_4$ nanocrystals as well. Furthermore there are two other possibilities which can be discounted: 1) different sizes of nanocrystals (mixture of big and small due to poor size dispersion); 2) presence of cubic phase nanocrystals along with hexagonal phase. Theoretically both these could provide a second doublet from the Y^{3+} ions, however, the second doublet's ratio with the main 3d doublet

would then not change with excitation energies. This also points out that the second peak is indeed from surface yttrium ions. We attribute the new chemical speciation observed for yttrium ions on the surface due to its interaction with the oleates which stabilize the nanocrystal and the fact that the crystal structure of the $NaYF_4$ is abruptly terminated. The yttrium ions on the inside are coordinated to fluoride ions while the surface yttrium ions are also coordinated with the oxygen(s) from the oleates. Oxygen is less electronegative than fluorine which could be the reason why the surface yttrium ions (second peak) have a slightly lower binding energy than yttrium ions inside the nanocrystal.

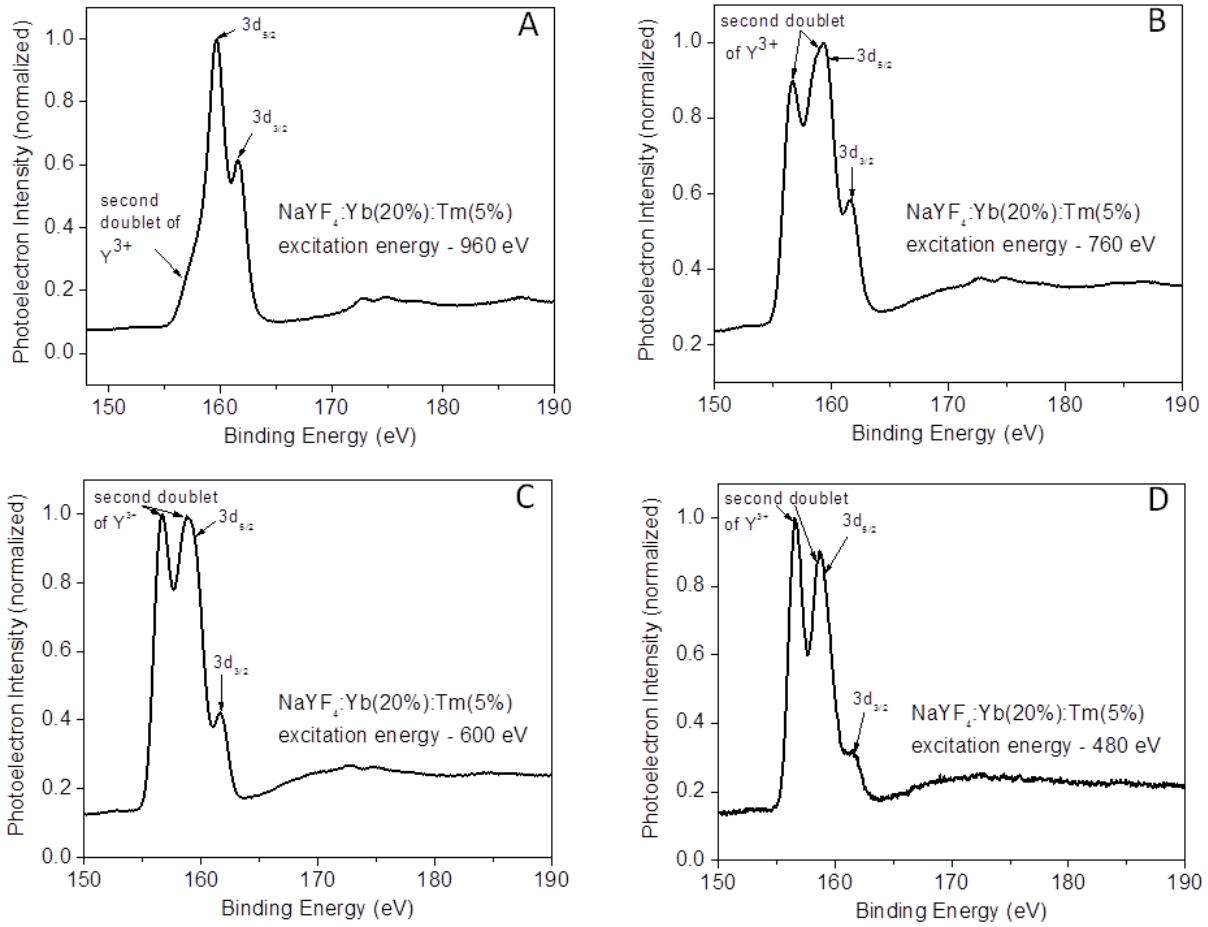

Figure 3. XPS spectra of $NaYF_4$ nanocrystals doped with Yb^{3+} and Tm^{3+} ions at different excitation energies. (A) The second peak around 157.5 eV for Y^{3+} ions is observed as a shoulder

to the main peak around 160 eV. (B-D) Second peak around 157.5 eV is clearly observed when compared to the main peak around 160 eV for yttrium ions.

When the core/shell $NaYF_4/NaYbF_4$ and $NaYF_4/NaTmF_4$ nanocrystals were analyzed with XPS we found other peaks other than arising from yttrium. The peaks around 178 to 220 eV for the core/shell $NaYF_4/NaTmF_4$ nanocrystal belong to the 4d peaks of thulium ions. In case of $NaYF_4/NaYbF_4$ nanocrystal the peaks around 187 to 220 eV belong to the 4d peaks of ytterbium ions. This was further confirmed by comparing an undoped $NaYF_4$ with $NaYF_4/NaTmF_4$ core/shell (Figure 4D). These peaks have shifted towards higher binding energy when compared to ytterbium and thulium metals. The binding energy peaks observed here are higher than that observed previously for ytterbium oxide and thulium oxides.[26] This is because of the fact that Yb^{3+} and Tm^{3+} ions are bound to fluorides which is more electronegative than oxygen, hence the binding energy is higher than previously reported. The interesting factor to note is that this study was started with the primary goal of understanding the dopant distribution of lanthanides (Yb^{3+} and Tm^{3+} ions) in the $NaYF_4$ matrix. Surprisingly, no photoelectrons from the 4d orbitals of either Tm^{3+} or Yb^{3+} ions were observed when they were doped in the $NaYF_4$ matrix (Figure 4DFigure). This is something surprising as our group has recently published results on LaF_3 nanocrystals doped with Gd^{3+} or Nd^{3+} ions and $NaGdF_4$ nanocrystals doped with Y^{3+} or Tb^{3+} or Nd^{3+} ions.[24] The doping level in $NaGdF_4$ nanocrystals were at 20 atom percent. There are two possibilities for the absence of signal: 1) The doped lanthanides could be buried deep inside the nanocrystals that 4d photoelectrons cannot escape due to the limited mean free escape path of the photoelectrons; 2) If the Yb^{3+} or Tm^{3+} ions are isotropically distributed in the $NaYF_4$ nanocrystal we can generate 4d photoelectrons from the lanthanides. However, the number of 4d photoelectrons generated might not be large enough to obtain a signal above the background

noise. Our future work will involve in understanding the growth mechanism of these nanocrystals i.e. the precipitation of lanthanides in combination with yttrium ions in the organic phase at high temperatures. The process of precipitation of lanthanides has been shown to be very complex in aqueous system, where all the lanthanides precipitate almost at the same time; however they get exchanged with each other after that. Hence we expect a similar situation in the organic phase and understanding the kinetics of the lanthanide precipitation will provide us data to arrive at a conclusion on how these elements are doped inside the nanocrystal. This could also probably shed light on the fact on why we do not observe any signal from Yb^{3+}, and Tm^{3+} ions when they are doped inside $NaYF_4$ nanocrystals.

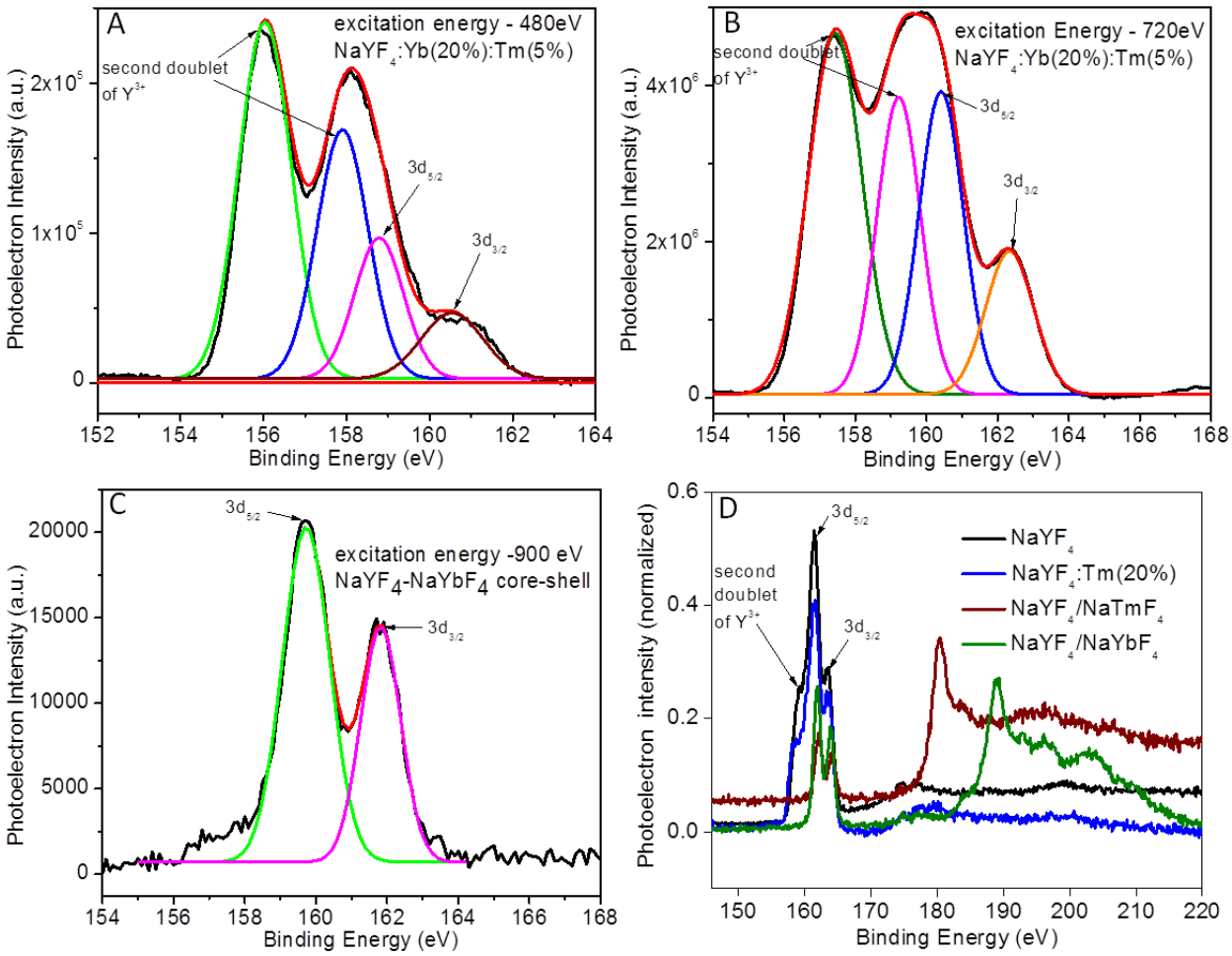

Figure 4 (A & B) XPS spectra of $NaYF_4$ nanocrystals doped with Yb^{3+} and Tm^{3+} ions fitted with origin software to deconvolute the two doublets observed for yttrium ions. (C) XPS spectrum of $NaYF_4$- $NaYbF_4$ core-shell nanocrystals fitted with origin software. (D) XPS spectra of core/shell samples showing signals for Yb^{3+} and Tm^{3+}. The peaks from 181 to 195 eV present in $NaYF_4/NaTmF_4$ belong to 4d photoelectrons of Tm^{3+} ions. The peaks from 190 to 204 eV in $NaYF_4/NaYbF_4$ belong to 4d photoelectrons of Yb^{3+} ions. The subtle shift in the peaks around 175 to 180 eV observed between undoped $NaYF_4$ and $NaYF_4$:Tm(20%) is attributed to the instrument work function.

Conclusions

We found that surface yttrium ions are different from their counterparts inside the nanocrystal. This was identified from the high resolution XPS measurements which showed that there is a second doublet around 157.5 eV in addition to the first doublet observed for yttrium ions around 160 eV. We were also able to deduce the fact that the different chemical speciation was observed due to the surface yttriums being different from their counterpart inside the nanocrystal. This was found from the fact that the second doublet's intensity increased with respect to the other doublet as the excitation energy is decreased. The fact that surface yttrium ions exhibited a different chemical speciation was further confirmed when the second doublet disappeared with the growth of $NaYbF_4$ or $NaTmF_4$ shell over $NaYF_4$ nanocrystal. This is a very generic tool to investigate whether the dopants ions or the host matrix is on the surface. One example is if we codope two lanthanide ions we could in principle figure out whether they are close to each other or spatially separated and which one is on the surface. This will be very significant if we either want to improve the energy transfer between the two dopants or spatially separate them. Hence we believe this fundamental investigation will aid in future studies to understand more about the structure and the surface of (doped) lanthanide-based nanocrystals.

Experimental Details

Synthesis of hexagonal (β–phase) $NaYF_4$ and $NaYF_4$:Yb(20%):Tm(5%) nanocrystals

Yttrium chloride (0.75 millimole), ytterbium chloride (0.20 millimole), thulium chloride (0.05 millimole) were mixed with 6 ml of oleic acid and 15 ml of octadecene and heated to 110 ^{o}C under vacuum and maintained at that temperature for 2 hours to form the oleate complexes. The reaction was brought to room temperature followed by addition of NaOH (0.100 millimole) and

NH_4F (0.148 millimole) in 10 ml of methanol. The reaction mixture was stirred for 30 minutes followed by the evaporation of methanol under a stream of argon at 55 - 60 ^oC. Once the methanol was completely evaporated, the reaction mixture was heated to 297 ± 2 ^oC and maintained at that temperature for 1 hour under a steady argon flow. Following this the reaction mixture was cooled to room temperature the nanocrystals were precipitated from the reaction mixture using ethanol (100%). The precipitated nanocrystals were dispersed in 3 ml of hexane followed by reprecipitation in ethanol (25 ml). This process was done once more to wash the nanocrystals. The washed nanocrystals were then dried under a stream of air for 20 to 30 sec and dispersed in hexane. For undoped $NaYF_4$ nanocrystals the same procedure was followed.

Synthesis of $NaYF_4$/$NaYbF_4$ and $NaYF_4$/$NaTmF_4$ nanocrystals

This synthesis was carried out on the basis of Yan et.al.[27] and our group's previous publication.[28] In order to make core/shell nanocrystals the shell material (cubic nanocrystals) was pre-synthesized. Ytterbium oxide (1 millimole) was mixed with 20 ml of 50% aqueous trifluoroacetic acid and refluxed at 85 ^oC overnight. Following this, the excess trifluoroacetic acid and water was removed by heating the mixture at 65 ^oC to obtain a white powder. The white precursor powder was taken in a three necked flask with sodium trifluoroacetate (2 millimoles), oleylamine (6 ml), oleic acid (6 ml), and octadecene (10 ml) and heated at 120 ^oC for 45 minutes under vacuum. This was done to remove any excess water, and trifluoroacetic acid. After 45 minutes at 120 ^oC under vacuum the reaction mixture was heated to 290 ^oC under a flowing stream of argon at 15 ^oC/min. The reaction mixture was stirred vigorously at 290 ^oC for 45 minutes and then cooled to room temperature. The nanocrystals were precipitated using 50 ml of ethanol (100%) and then washed twice more. The nanocrystals were finally dispersed in hexanes. These nanocrystals are used as the material for the shell growth. The core $NaYF_4$ nanocrystals

synthesis was followed as in the previous section till heating to 297 ± 2 ^{o}C. The reaction was continued for 60 minutes at 297 ± 2 ^{o}C after which the cubic nanocrystals were injected into the core nanocrystal's solution. The temperature drops between 285 - 290 ^{o}C when the cubic nanocrystals are injected. The reaction was allowed to continue for 10 minutes after the injection followed by cooling the reaction to room temperature. The washing procedure was the same as the core nanocrystal synthesis. The samples were finally dispersed in hexane. The same procedure is followed for $NaYF_4$/$NaTmF_4$ nanocrystals.

Energy-dependent X-ray photoelectron spectroscopy

These experiments were carried out with the synchrotron light source at the Canadian Light Source Inc. The samples were prepared by drop-casting the nanocrystals hexane dispersions on to a thin gold foil. The gold foil was mounted on a sample holder using a double sided tape. The gold foil was used for two purposes: 1) reference material; 2) reduce the charging of the sample. The sample holder is mounted inside the sample chamber which is under 10^{-6} Torr vacuum. The measurements were carried out at the Spherical Grating Monochromator (SGM) beamline at the Canadian light Source. Different excitation photon energies were used for depth profiling of the samples. The photoelectron peaks from gold is used as the reference spectrum.

Transmission Electron Microscopy

The TEM images of the QDs were obtained using a JEOL 1400 instrument operating at 80 kV equipped with a charge-coupled device (CCD) camera. The QDs dispersed in hexane were drop-casted onto a carbon coated formvar grid and dried under air.

X-ray Diffraction

XRD patterns were measured with Cr (30 kV, 15 mA) radiation on a Rigaku Miniflex diffractometer using a zero-background holder with variable divergence slit, 4.2° scattering slit, and 0.3 mm receiving slit. The scanning step size is 0.5°, 2θ with a counting time of 2 s per step over the range of 20-140°. The dispersion was added drop wise to form a film on the substrate which was then used for the measurements. The peaks at 45^{o} and 48^{o} (Fig. S2) were used to confirm the size of the nanocrystals using Scherrer's equation.

Peak Fitting

The peak fitting in Figure 4 has been done using the software Origin Pro. Background correction was done before fitting the curve. The fitting was done using a polynomial equation as shown in the supporting information. The doublet from the 3d photoelectrons of yttrium ions in $NaYF_4$/$NaYbF_4$ (Figure 4C) were fitted with the position of the peaks as a constant while the area under the peak was changed. Following this, the same conditions were employed for fitting the convoluted peaks in Figure 4A&B. The fitting parameters are shown in SI table 1, 2 and 3.

Acknowledgements:

This work was supported by National Science and Engineering Research Council (NSERC) and Canadian Light Source (CLS), Saskatoon.

Supporting Information Available:

Figure S1 shows the XPS spectrum of gold. Figure S2 – S5 shows the energy-dependent XPS spectrum at different excitation energies for $NaYbF_4$:Yb:Tm. Figure S6 & S7 shows the TEM of $NaYF_4$-$NaTmF_4$ and $NaYF_4$-$NaYbF_4$ core-shell nanocrystals respectively. The details of the fitting parameters for $NaYF_4$:Yb(20%):Tm(2%) at excitation energies of 480 and 720 eV is

presented in table 1 & 2. All these materials can be obtained free of charge via the internet at http://pubs.acs.org.

References:

1. Alivisatos, A. P., Semiconductor Clusters, Nanocrystals, and Quantum Dots *Science* **1996**, *271*, 933-937.

2. Raymond, K. N.; Pierre, V. C., Next Generation, High Relaxivity Gadolinium MRI Agents *Bioconjugate Chem.* **2005**, *16*, 3-8.

3. Klimov, V. I., *Nanocrystal Quantum Dots*; Taylor and Francis Group, LLC: Boca Raton, 2010.

4. Wang, F.; Banerjee, D.; Liu, Y. S.; Chen, X. Y.; Liu, X. G., Upconversion Nanoparticles in Biological Labeling, Imaging, and Therapy *Analyst* **2010**, *135*, 1839-1854.

5. Wang, F.; Liu, X. G., Recent Advances in the Chemistry of Lanthanide-Doped Upconversion Nanocrystals *Chem. Soc. Rev.* **2009**, *38*, 976-989.

6. Auzel, F., Upconversion and Anti-Stokes Processes with f and d Ions in Solids *Chem. Rev.* **2004**, *104*, 139-173.

7. Auzel, F.; Pecile, D., Absolute Efficiency for IR to Blue Conversion Materials and Theoretical Prediction for Optimized Matrixes *J. Lumin.* **1976**, *11*, 321-30.

8. Menyuk, N.; Pierce, J. W.; Dwight, K., $NaYF_4$-Yb,Er - Efficient Upconversion Phosphor *Appl. Phys. Lett.* **1972**, *21*, 159-161.

9. Kobayashi, H.; Kosaka, N.; Ogawa, M.; Morgan, N. Y.; Smith, P. D.; Murray, C. B.; Ye, X. C.; Collins, J.; Kumar, G. A.; Bell, H., et al., In vivo multiple color lymphatic imaging using upconverting nanocrystals *J. Mater. Chem.* **2009**, *19*, 6481-6484.

10. Nyk, M.; Kumar, R.; Ohulchanskyy, T. Y.; Bergey, E. J.; Prasad, P. N., High Contrast In Vitro and In Vivo Photoluminescence Bioimaging Using Near Infrared to Near Infrared

Up-Conversion in Tm^{3+} and Yb^{3+} Doped Fluoride Nanophosphors *Nano Lett.* **2008**, *8*, 3834-3838.

11. Pichaandi, J.; Boyer, J. C.; Delaney, K. R.; van Veggel, F. C. J. M., Two-Photon Upconversion Laser (Scanning and Wide-Field) Microscopy Using Ln^{3+}-Doped $NaYF_4$ Upconverting Nanocrystals: A Critical Evaluation of their Performance and Potential in Bioimaging *J. Phys. Chem. C* **2011**, *115*, 19054-19064.

12. Gai, S. L.; Li, C. X.; Yang, P. P.; Lin, J., Recent Progress in Rare Earth Micro/Nanocrystals: Soft Chemical Synthesis, Luminescent Properties, and Biomedical Applications *Chem. Rev.* **2014**, *114*, 2343-2389.

13. Li, C. X.; Lin, J., Rare earth fluoride nano-/microcrystals: synthesis, surface modification and application *J. Mater. Chem.* **2010**, *20*, 6831-6847.

14. Sudarsan, V.; van Veggel, F. C. J. M.; Herring, R. A.; Raudsepp, M., Surface Eu^{3+} Ions Are Different Than "Bulk" Eu^{3+} Ions in Crystalline Doped LaF_3 Nanoparticles *J. Mater. Chem.* **2005**, *15*, 1332-1342.

15. Wang, F.; Wang, J. A.; Liu, X. G., Direct Evidence of a Surface Quenching Effect on Size-Dependent Luminescence of Upconversion Nanoparticles *Angew. Chem. Int. Ed.* **2010**, *49*, 7456-7460.

16. Vetrone, F.; Naccache, R.; Mahalingam, V.; Morgan, C. G.; Capobianco, J. A., The Active-Core/Active-Shell Approach: A Strategy to Enhance the Upconversion Luminescence in Lanthanide-Doped Nanoparticles *Adv. Funct. Mater.* **2009**, *19*, 2924-2929.

17. Henderson, G. S.; Baker, D. R., *Synchrotron Radiation: Earth, Environmental and Material Sciences Applications*; Mineralogical Association of Canada: Saskatoon, 2002; Vol. 30.

18. Borchert, H.; Haubold, S.; Haase, M.; Weller, H., Investigation of ZnS Passivated InP Nanocrystals by XPS *Nano Lett.* **2002**, *2*, 151-154.

19. McGinley, C.; Borchert, H.; Talapin, D. V.; Adam, S.; Lobo, A.; de Castro, A. R. B.; Haase, M.; Weller, H.; Möller, T., Core-level Photoemission Study of the InAs/CdSe Nanocrystalline System *Phys. Rev. B* **2004**, *69*, 045301/1-045301/6.

20. Shard, A. G., A Straightforward Method For Interpreting XPS Data From Core-Shell Nanoparticles *J. Phys. Chem. C* **2012**, *116*, 16806-16813.

21. Abel, K. A.; Boyer, J.-C.; van Veggel, F. C. J. M., Hard Proof of the $NaYF_4$/$NaGdF_4$ Nanocrystal Core/Shell Structure *J. Am. Chem. Soc.* **2009**, *131*, 14644-14645.

22. Battocchio, C.; Porcaro, F.; Mukherjee, S.; Magnano, E.; Nappini, S.; Fratoddi, I.; Quintiliani, M.; Russo, M. V.; Polzonetti, G., Gold Nanoparticles Stabilized with Aromatic Thiols: Interaction at the Molecule-Metal Interface and Ligand Arrangement in the Molecular Shell Investigated by SR-XPS and NEXAFS *J. Phys. Chem. C* **2014**, *118*, 8159-8168.

23. Dong, C. H.; Pichaandi, J.; Regier, T.; van Veggel, F. C. J. M., The Unexpected Structures of "Core-Shell" and "Alloy" LnF_3 Nanoparticles as Examined by Variable Energy X-ray Photo-Electron Spectroscopy *Nanoscale* **2011**, *3*, 3376-3384.

24. Dong, C.; Pichaandi, J.; Regier, T.; van Veggel, F. C. J. M., Nonstatistical Dopant Distribution of Ln^{3+}-Doped $NaGdF_4$ Nanoparticles *J. Phys. Chem. C* **2011**, *115*, 15950-15958.

25. Jiang, G. C.; Pichaandi, J.; Johnson, N. J. J.; Burke, R. D.; van Veggel, F. C. J. M., An Effective Polymer Cross-Linking Strategy To Obtain Stable Dispersions of Upconverting $NaYF_4$ Nanoparticles in Buffers and Biological Growth Media for Biolabeling Applications *Langmuir* **2012**, *28*, 3239-3247.

26. Lang, W. C.; Padalia, B. D.; Watson, L. M.; Fabian, D. J.; Norris, P. R., Multiplet Structure in X-Ray Photoelectron-Spectra of Rare-Earth Elements and Their Surface Oxides *Faraday Discuss* **1975**, *60*, 37-43.

27. Mai, H. X.; Zhang, Y. W.; Sun, L. D.; Yan, C. R., Size- and Phase-Controlled Synthesis of Monodisperse $NaYF_4$: Yb,Er Nanocrystals from a Unique Delayed Nucleation

Pathway Monitored with Upconversion Spectroscopy *J. Phys. Chem. C* **2007**, *111*, 13730-13739.

28. Johnson, N. J. J.; Korinek, A.; Dong, C. H.; van Veggel, F. C. J. M., Self-Focusing by Ostwald Ripening: A Strategy for Layer-by-Layer Epitaxial Growth on Upconverting Nanocrystals *J. Am. Chem. Soc.* **2012**, *134*, 11068-11071.

TOC

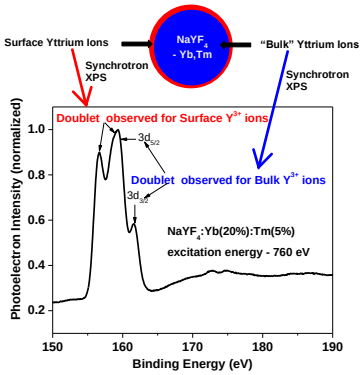
Surface Yttrium Ions
NaYF4 - Yb,Tm
"Bulk" Yttrium Ions
Synchrotron XPS
Synchrotron XPS
Doublet observed for Surface Y3+ ions
3d5/2
Doublet observed for Bulk Y3+ ions
3d3/2
NaYF4:Yb(20%):Tm(5%)
excitation energy - 760 eV
Photoelectron Intensity (normalized)
1.0
0.8
0.6
0.4
0.2
150
160
170
180
190
Binding Energy (eV)